

FREQUENCY COMPARISON (H_MASER 40 0890) - (LNE-SYRTE-FO2)
During the period MJD 54069 to MJD 54079
&
During the period MJD 54089 to MJD 54094

The primary frequency standard LNE-SYRTE-FO2 in Caesium mode was compared to the hydrogen Maser (40 0890) of the laboratory during the 30th November to 10th December 2006 (MJD 54069 to MJD 54079) and during 20th to 25th December 2006 (MJD 54089 to MJD 54094).

Period (MJD)	y(HMaser _{40 0890} - FO2)	u_B	u_A	$u_{link / maser}$
54069 – 54079	- 3770,5	3.8	1,1	1,5
54089 – 54094	- 3800,1	4.1	6,9	1,7

Table 1: Results of the comparison in 1×10^{-16} .

The measurements of fractional frequency differences are corrected for the systematic frequency shifts listed below. Figure 1 shows the averaged frequencies measurements during December.

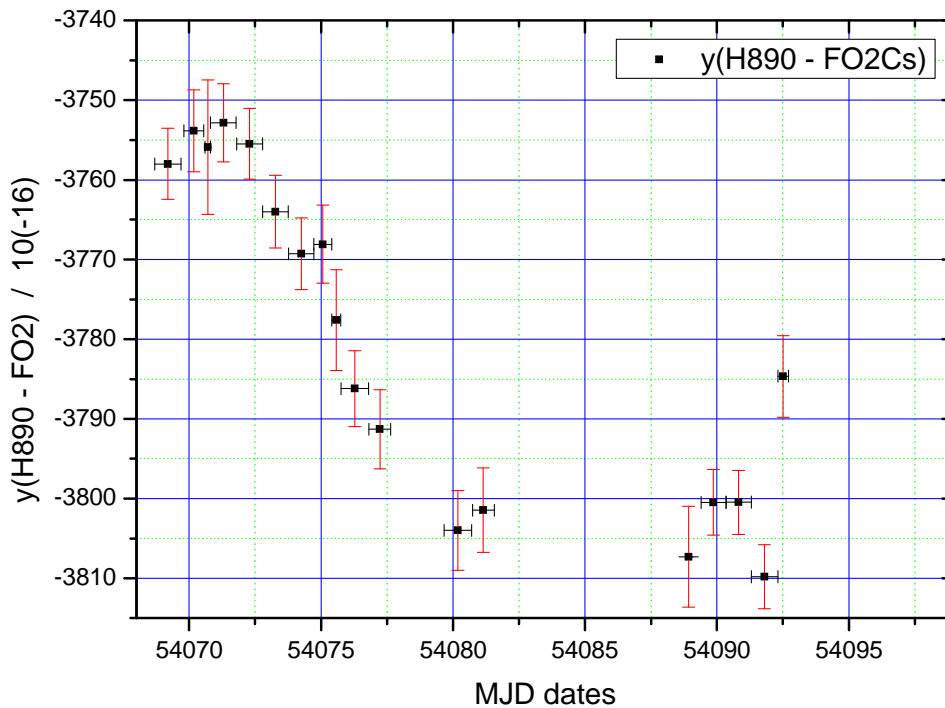


Figure 1: Fractional frequency differences H890-FO2 December period

Frequency average between the Maser 40 0890 and the SYRTE fountain FO2

Frequency measurements averaged of FO2 fountains were fitted over the period MJD 54069 to 54079 by a polynomial fit order 5. Figure 2 shows the overlapping frequency averaged measurements (blue stars) and the polynomial fit (red line). The frequency difference between Maser 40 0890 and FO2 fountain was calculated by integrating the polynomial fit over the period MJD 54069 to MJD 54079 and gives -3770.5×10^{-16} . For the period MJD 54089 to 54094 a linear fit was used with extrapolated frequency at the beginning and the ending of this period. Figure 3 shows the frequency measurements averaged over time interval of 12H assorted by their statistical uncertainty and the frequency estimation at the limit of this period assorted by a larger statistical uncertainty issued from confidence bounds. The frequency average over the period MJD 54089-54094 is given by the frequency of the linear fit at the middle date of the period and we obtain -3800.9×10^{-16} .

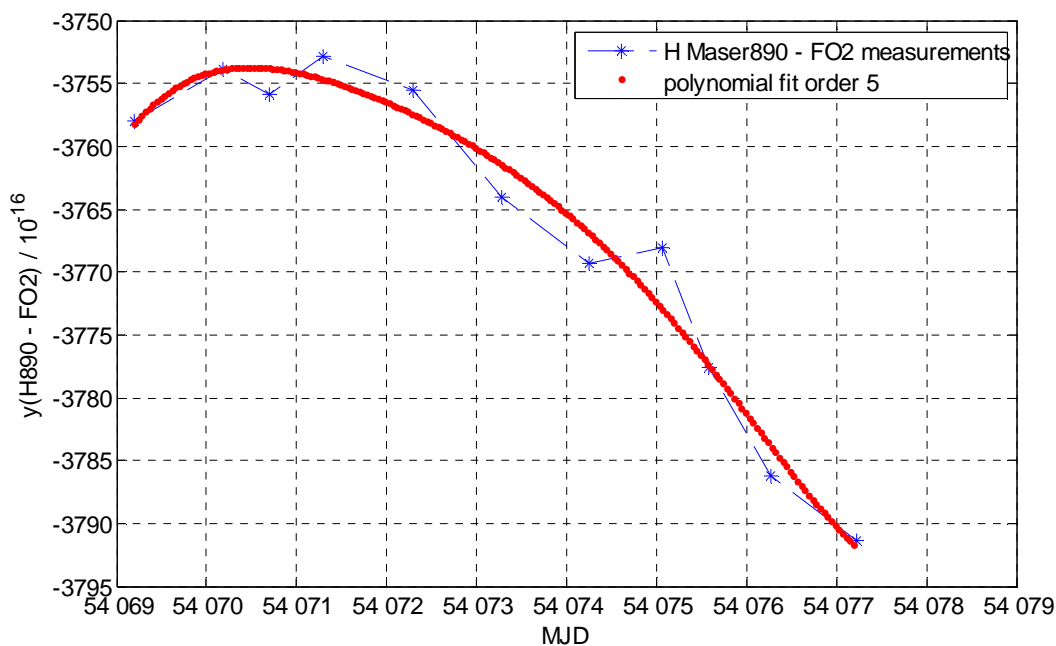


Figure 2: polynomial regression used to estimate the frequency average during period 54069-54079 of FO2 measurements

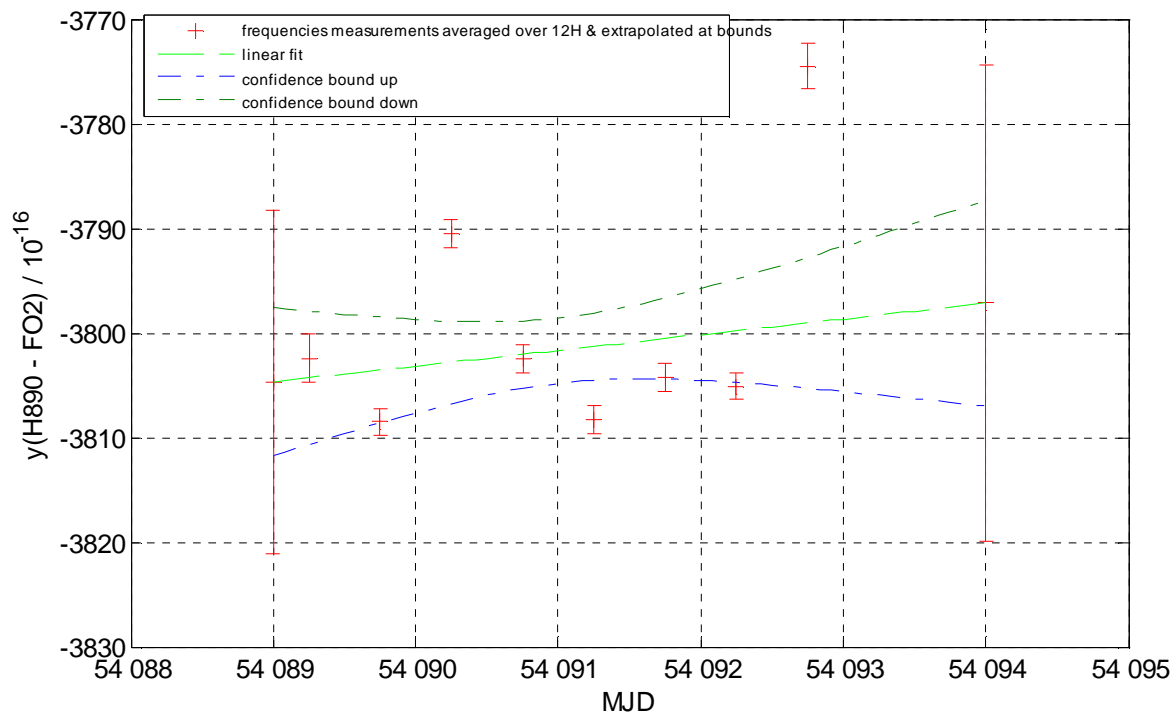


Figure 3: linear regression used to estimate the frequency average during period 54089-54095 of FO2 measurements

Statistical uncertainty on FO2 measurements

Statistical uncertainty $\sigma_A = u_A$, is calculated with the statistical uncertainty on each measurement σ_{Stat_i} and statistical effect on the cold collisions and Cavity Pulling measurement $\sigma_{Collision_i}$:

$$\sigma_A = \sqrt{\frac{1}{\sum_{i=1}^n \frac{1}{\sigma_{Stat_i}^2 + \sigma_{Collision_i}^2}}}$$

We found for the period MJD 54069 to MJD 54079

$$u_A = 1.14 \times 10^{-16}$$

And for the period MJD 54089 to MJD 54094, the uncertainty associated with this method of frequency average estimation is evaluated using the confidence bounds corresponding to +/- 1 σ over the linear fit.

We found for the period MJD 54084 to MJD 54099

$$u_A = 6.92 \times 10^{-16}$$

Uncertainty due to the dead times and due to the link between Maser890 and the fountain FO2

Uncertainties due to the dead time were calculated by stability analyses of Maser 40 0890 with respect to the Maser 40 0889 during the December 2006. Figure 4 gives the fluctuation frequency differences between Maser 40 0890 and Maser 40 0889 during the period of December. These uncertainties were extrapolated from the time deviation between Maser 40 0890 and 40 0889 for each dead time duration observed during this period of FO2 measurements. We found for the period MJD 54069 to MJD 54079 $\sigma_{Dead_Time} = 1.11 \times 10^{-16}$ and for the period MJD 54089 to MJD 54094 $\sigma_{Dead_Time} = 1.35 \times 10^{-16}$

Uncertainty due to the link between Maser890 and the fountain FO2 is

$$u_{link_Maser} = \sqrt{\sigma_{link_Lab}^2 + \sigma_{dead_time}^2}$$

With $\sigma_{link_Lab} = 1.0 \times 10^{-16}$, the uncertainty due to the dead times during the period MJD 54069 to MJD 54079 obtained is:

$$u_{Link / Maser} = 1.49 \times 10^{-16}$$

And for the period MJD 54089 to MJD 54094

$$u_{Link / Maser} = 1.68 \times 10^{-16}$$

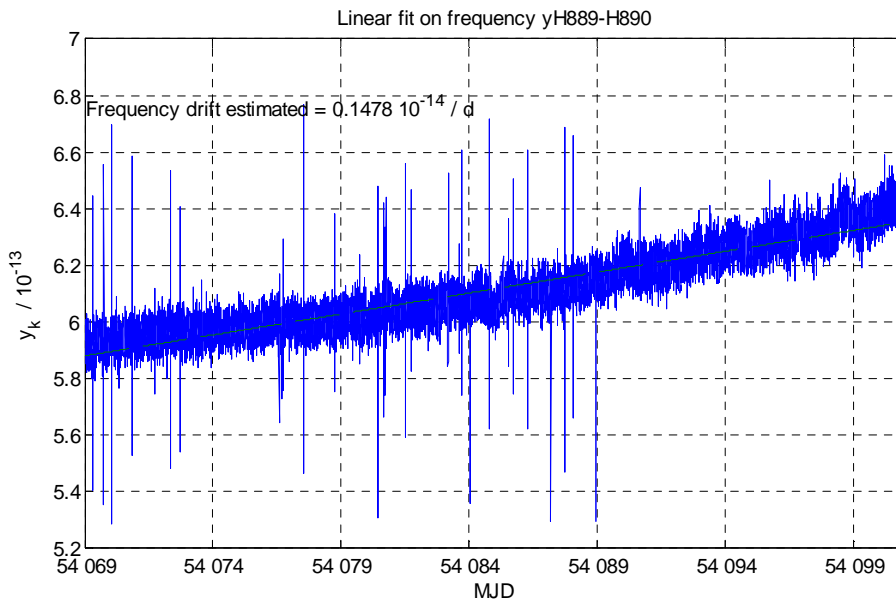


Figure 4: fluctuation frequency differences Maser890 with respect to Maser889

Uncertainties budget of systematic effects in the FO2 fountain

Systematic effects taken into account are the quadratic Zeeman, the Black Body, the cold collision and cavity pulling corresponding to the systematic part, the microwave spectral purity and the microwave leakage, the Ramsey Rabi pulling, the recoil, the 1st and 2nd Doppler and the background collisions. Each of these effects is affected by an uncertainty. The uncertainty of the red shift effect is also included in the systematic uncertainty budget. Systematic uncertainty is estimated by the sum of quadratic systematic uncertainties and gives

$$\sigma_B = \left(\sigma_{Zeeman}^2 + \sigma_{BlackBody}^2 + \sigma_{Collision_{Syst}}^2 + \sigma_{Microwave_Spectrum_Leakage}^2 + \sigma_{first_Doppler}^2 + \sigma_{Ramsey_Rabi}^2 + \sigma_{Recoil}^2 + \sigma_{second_Doppler}^2 + \sigma_{Background_collisions}^2 + \sigma_{Redshift}^2 \right)^{(1/2)}$$

Table 2 resumes the budget of systematic effects and their associated uncertainties. More details on systematic effects are developed in the next paragraphs.

	Correction (10 ⁻¹⁶)	Uncertainty (10 ⁻¹⁶)	Correction (10 ⁻¹⁶)	Uncertainty (10 ⁻¹⁶)
Quadratic Zeeman effect	- 1920.4	0.1	- 1920.5	0.14
Black body radiation	168.7	0.6	168.1	0.6
Cold collisions and cavity pulling	115.3	1.1	168.3	1.7
Microwave spectral purity & leakage		0.5		0.5
Ramsey & Rabi pulling		< 0.1		< 0.1
Microwave recoil		< 1.4		< 1.4
First order Doppler effect		3.0		3.0
Second order Doppler effect		< 0.1		< 0.1
Background gas collisions		<1.0		<1.0
Total		3.71		3.94
Red shift	- 65.4	1.0	- 65.4	1.0
Total with red shift		3.84		4.06

Table 2: budget of systematic effects and uncertainties for SYRTE-FO2 fountain

For the December 2006 the two periods MJD 54069-54079 and MJD 54089-54094 we obtain

$\sigma_B = 3.8 \cdot 10^{-16}$	$\sigma_B = 4.1 \cdot 10^{-16}$
---------------------------------	---------------------------------

1 - Measurement of the 2nd order Zeeman frequency shift

Every 20 minutes the frequency of the central fringe of the field linearly dependant transition $|F=3, m_F=1\rangle \rightarrow |F=4, m_F=1\rangle$ is measured. This frequency is directly proportional to the field as $\delta(\nu_{11})=K_{Z1}B$ with $K_{Z1} = 7,0084 \text{ Hz.nT}^{-1}$ (see [5] vol. 1 p37 table 1.1.7(a)). In the fountain, the transition $|F=3, m_F=0\rangle \rightarrow |F=4, m_F=0\rangle$ is shifted by quadratic Zeeman effect and depend on squared magnetic field as $\delta(\nu_{00})=K_{Z2}B^2$ with $K_{Z2} = 42,745 \text{ mHz.}\mu\text{T}^{-2}$ (see [5] vol. 1 p37 table 1.1.7(a)). Knowing K_{Z1} and

measuring $\delta(\nu_{11})$ allow good estimation of Zeeman quadratic shift as $\delta(\nu_{00}) = K_{Z2} \left(\frac{\delta(\nu_{11})}{K_{Z1}} \right)^2$. The

relative quadratic Zeeman frequency shift is calculated by $\frac{\delta(\nu_{00})}{\nu_0} = \frac{427,45 \times 10^{-6} \left(\frac{\delta(\nu_{11})}{700,84} \right)}{\nu_0}$ with $\delta(\nu_{11})$ in Hz unit and $\nu_0 = 9192631770$ Hz. And the uncertainty is evaluated by $\frac{\Delta(\delta(\nu_{00}))}{\nu_0} = 427,45 \times 10^{-6} \times \frac{2 \times \bar{B} \times \Delta(B)}{\nu_0}$ with B in mG and $\Delta(B)$ the standard deviation of the magnetic field.

The tracking of the central fringe during December shows the good stability of the magnetic field in the interrogation zone. The frequency variation is taken in the time interval 54069 to 54079, as the standard deviation ± 0.03598345368 Hz and ± 0.0505543388 Hz during the period MJD 54089-54094. When taking the standard deviation of variation of the magnetic field $\Delta(B)$ over the whole period of measurement as the field uncertainty, we find **5.134 pT** and **7.213 pT** respectively during the first and last December periods. The corresponding uncertainty of the correction of the second order Zeeman effect is **9.7×10^{-18}** and **13.6×10^{-18}** respectively during the first and last December periods. During each period of about 24h of integration an evaluation of the Zeeman effect is calculated assorted with an uncertainty averaged from the tracking of the central fringe during this interval duration of about 24h. For the central fringe $M1 = 1424.28098258493$ Hz and $M1 = 1424.33103056225$ Hz respectively during

the first and last December periods, the relative quadratic Zeeman shift is $\frac{\delta(f)_{Zeeman2}}{\nu_0} = \frac{K_{Z2} M1^2}{K_{Z1}^2 \nu_0}$

Frequency quadratic Zeeman shift was evaluated respectively for the two periods of December:

$$\frac{\delta(f)_{Zeeman2}}{\nu_0} = 1.9204 \times 10^{-13} / 1.9205 \times 10^{-13}$$

The associated uncertainty of the quadratic Zeeman shift was calculated for the two periods of December

$\sigma_{Zeeman2} = 9.703 \cdot 10^{-18}$	$\sigma_{Zeeman2} = 13.63 \cdot 10^{-18}$
---	---

2 - Measurement of the collisional frequency shift and the cavity pulling

Collisional shift takes into account the effect of the collisions between cold Caesium atoms and the effect of "Cavity Pulling" whose influence also depends on the number of atoms. This effect is measured in a differential way during each integration and its determination thus depends on the duration of the measurement and on the stability of the clock, thus the uncertainty on the determination of the collisional shift is mainly of statistical nature. To the statistical uncertainty, we add a type B uncertainty of 1% of frequency shift resulting from the imperfection of the adiabatic passage method (see [4]).

The relative frequency shift due to the effect of the collisions and "Cavity Pulling" of the atomic fountain FO2 were measured in low density, between the MJD 54069 and 54079 and between the MJD 54089 to MJD 54094 with the statistical uncertainty, $\sigma_{Collision(i)}$.

The stability of a differential measurement using high and half atom density fountain configurations during MJD 54069 to MJD 54079 and during MJD 54089 to MJD 54094 using the Allan deviation was calculated, in order to correct of the cold collisional shift for this period. FO2 was operated alternatively (every 50 clock cycles) at low atomic density and high density against the cryogenic oscillator weakly phase locked on the Hydrogen Maser 40 0890. The measured density ratio between low and high densities is **0.50015486 ± 0.000262** for the first period of December and **0.50012089 ± 0.000132** for the second period of December. The frequency difference between both densities is used to determine the

collisional coefficient which is used to correct each data point. The Allan deviation varies as $\tau^{-1/2}$ and reaches 10^{-16} after 100000s.

The weighted mean $y_{Collision\ moy} = \frac{\sum_{i=1}^n \frac{y_{Collision\ i}}{2}}{\sum_{i=1}^n \frac{1}{2\sigma_{Collision\ i}}}$ of collisional shift gives for the December 2006 period

MJD 54069 to MJD 54079:

$$y_{Collision\ moy} := -1.1537 \cdot 10^{-14}$$

MJD 54089 to MJD 54094:

$$y_{Collision\ moy} := -1.6834 \cdot 10^{-14}$$

The systematic effect of these shifts is evaluated by the 1% part of the mean frequency collisional shift during the two periods of December 2006, MJD 54069-54079 and MJD 54089-54094 are:

$$\sigma_{Collision\ Syst} = \frac{1}{100} |y_{Collision\ moy}| = \left[(\sigma_{Collision})_{Syst} = 1.1537 \cdot 10^{-16} \quad (\sigma_{Collision})_{Syst} = 1.6834 \cdot 10^{-16} \right]$$

This value is taking into account in the systematic uncertainty evaluation σ_B .

3 - Measurement of the Blackbody Radiation shift

An ensemble of 3 platinum thermistors monitors the temperature and its gradient inside the vacuum chamber. The average temperature is $T \sim 24,8^\circ\text{C}$ with a gradient smaller than $\delta(T) = 0.2\text{ K}$ along the atom trajectory. The correction is

$$\left(\frac{\delta(\nu)}{\nu_0} \right)_{BlackBody} = \frac{K_{BB} T^4 \left(1 + \frac{\epsilon T^2}{T_0^2} \right)}{T_0^4}$$

with $K_{BB} = -1.573 \times 10^{-4} \pm 3 \times 10^{-7}$ [10], $\epsilon := 0.014 \pm -0.0014$ [11],[12], $T_0 := 300\text{ K}$. The

Blackbody Radiation shift is assorted of uncertainty obtained with the squared of quadratic sum of $\delta(K_{BB})$, $\delta(\epsilon)$ and $\delta(T)$:

$$\left(\frac{\delta(\nu)}{\nu_0} \right)_{BlackBody} = -1.6875 \times 10^{-14} \pm 0.6 \times 10^{-16}$$

4 - Effect of the Microwave Spectrum effect and leakage effect

Microwave leaks are strongly suppressed (smaller than 10^{-17}) by switching the microwave field off by 40 dB when the atomic cloud is outside the Ramsey cavity. The microwave switch has been specifically developed and tested for this application [10]. Systematic effect related to a putative residual phase transient introduced by the switch is estimated to be smaller than 3×10^{-17} . Other effects related to the microwave synthesis have been assessed through phase noise power spectral density measurements, comparisons between synthesizers with strongly different synthesis schemes, *in situ* phase transient analysis, as reported in [11]. The corresponding uncertainty is 4×10^{-17} . The overall uncertainty connecting to microwave related issues is 5×10^{-17} .

$$\left(\frac{\delta(\nu)}{\nu_0} \right)_{\text{MicrowaveSpectrum}} = 0 \pm 0.5 \times 10^{-16}$$

5 - Measurement of the residual 1st order Doppler effect

We determined the frequency shifts caused by asymmetry of the coupling coefficients of the two microwave feedthroughs and the error on the launching direction by coupling the interrogation signal either “from the right” or “from the left” or symmetrically into the cavity. The measured shift is

$$\left(\frac{\delta(\nu)}{\nu_0} \right)_{\text{FirstDoppler}} = 0 \pm 3.0 \times 10^{-16}$$

In FO2 fountain we feed the cavity symmetrically at 1% level both in phase and in amplitude. This shift is thus reduced by a factor of 100 and became negligible. The quadratic dependence of the phase becomes dominant. A worse case estimate based on [6] gives fractional frequency shift of 3×10^{-16} which we take as uncertainty due to the residual 1st order Doppler effect.

6 – Rabi and Ramsey effect and Majorana transitions effect

An imbalance between the residual populations and coherences of $m_F < 0$ and $m_F > 0$ states can lead to a shift of the clock frequency estimated to few 10^{-18} for a population imbalance of 10^{-3} that we observe in FO2 (see [7] and [8]).

7 – Microwave recoil effect

The shift due to the microwave photon recoil was investigated in [3]. It is smaller than $1,4 \times 10^{-16}$.

8 – Gravitational red-shift and 2nd order Doppler shift

The relativistic effect is evaluated as $\frac{(\delta(\nu))_{\text{redshift}}}{\nu_0} = \frac{g h}{c^2}$ with $h=60\text{m}$ $\frac{(\delta(\nu))_{\text{redshift}}}{\nu_0} = 6.540 \times 10^{-15}$

$$\pm \sigma_{\text{Redshift}} = 0.1 \times 10^{-15}$$

The 2nd order Doppler shift is less than $0,08 \times 10^{-16}$.

9 – Background collisions effect

The vacuum pressure inside the fountains is typically a few 10^{-8} Pa. Based on early measurements of pressure shift (see [5]) the frequency shift due to collisions with the background gas is $< 10^{-16}$.

REFERENCES

- [1] - C. Vian, P. Rosenbusch, H. Marion, S. Bize, L. Cacciapuoti, S. Zhang, M. Abgrall, D. Chambon, I. Maksimovic, P. Laurent, G. Santarelli, A. Clairon of Obs. Paris, SYRTE, A. Luiten, M. Tobar, Univ. W. of Australia School of Physics, C. Salomon of LKB, "LNE-SYRTE Fountains: Recent Results", **CPEM 2004, Proceedings IEEE Transactions on Instrumentation & Measurement, Vol. 54, N0. 2, April 2005.**
- [2] - F. Pereira Do Santos, H. Marion, M. Abgrall, S. Zhang, Y. Sortais, S. Bize, I. Maksimovic, D. Calonico, J. Grünert, C. Mandache, C. Vian, P. Rosenbusch, P. Lemonde, G. Santarelli, Ph. Laurent and A. Clairon of LNE-SYRTE, C. Salomon of LKB, "Rb and Cs Laser Cooled Clocks: Testing the Stability of Fundamental Constants". **Proceedings IEEE 2003, EFTF Tampa May 2003, p 55-67.**
- [3] - P. Wolf of LNE SYRTE, C.J. Bordé of LPL, "Recoil effects in microwave Ramsey spectroscopy", arxiv: **quant-ph/0403194.**
- [4] - F. Pereira Do Santos, H. Marion, S. Bize, Y. Sortais, A. Clairon, and C. Solomon "Controlling the Cold Collision Shift in High Precision Atomic Interferometry" of, **Phys, Rev, Lett, 89,233004 (2002).**
- [5] - J. Vanier, C. Audouin, « The Quantum Physics of Atomic Frequency Standards », **Adam Hilger, Bristol & Philadelphia (1989).**
- [6] - R. Schröder, U. Hübner and D. Griebisch, "Design and Realization of the Microwave Cavity in PTB Caesium Atomic Clock CSF1" **IEEE Trans. Instrum. Meas., vol. 49, p.383, 2002.**
- [7] - L. Cutler *et al*, "Frequency pulling by hyperfine σ - transitions in cesium atomic frequency standards, **J. Appl. Phys. Vol. 69, pp. 2780, 1991.**
- [8] - A. Bauch, R. Schröder "Frequency shift in Caesium Atomic Clock due to Majorana transitions", **Annalen der Physik, vol. 2, pp. 421, 1993.**
- [9] – H. Marion thèse de doctorat de l'Université de Paris 6 (Mars 2005)
- [10] - G. Santarelli *et al.*, Proceedings of the 2006 EFTF (2006).
- [11] - D. Chambon *et al.*, IEEE Trans. Ultrason. Ferroelect. Freq. Contr., *in press.*